Pauli spin blockade in double molecular magnets

Anna Płomińska* and Ireneusz Weymann
Faculty of Physics, Adam Mickiewicz University, 61-614 Poznań, Poland
(Received 21 April 2016; revised manuscript received 20 June 2016; published 15 July 2016)

The Pauli spin blockade effect in transport through two, coupled in series, single molecular magnets weakly attached to external leads is considered theoretically. By using the real-time diagrammatic technique in the lowest-order perturbation theory with respect to the coupling strength, the behavior of the current and the shot noise is studied in the nonlinear response regime. It is shown that the current suppression occurs due to the occupation of highest-weight spin states of the system. Moreover, transport properties are found to strongly depend on parameters of the double molecular magnet, such as the magnitude of spin, internal exchange interaction and the hopping between the molecules. It is also demonstrated that the current suppression may be accompanied by negative differential conductance and a large super-Poissonian shot noise. The mechanisms leading to those effects are discussed.

DOI: 10.1103/PhysRevB.94.035422

I. INTRODUCTION

Transport properties of individual large-spin molecules exhibiting magnetic anisotropy, such as single molecular magnets (SMMs), have recently attracted considerable attention [1–5]. This is due to the fact that such nanosystems are considered to be important for future information technology [6–8] and in molecular spintronics [5]. The current flowing through a single molecular magnet depends greatly on the intrinsic properties of the molecule and the quality of coupling to external leads [4]. When the coupling is relatively weak, single-electron charging effects become relevant [9–12], whereas in the strong coupling regime, the electronic correlations can give rise to the Kondo effect [13–18]. Transport characteristics of single magnetic molecules have already been extensively studied, both experimentally [19–29] and theoretically [30–36], and are thus relatively well-understood. However, this is not necessarily the case for more complex molecular structures, which can exhibit further interesting properties, such as current suppression and negative differential conductance (NDC) [37–39]. One important example is a system built of two single molecular magnets [40–46]. In particular, it was shown that by changing the orientation of magnetic moments of two molecules attached to metallic leads, one can generate a spin-valve-like effect, in which the magnitude of the current depends on the mutual orientation of SMMs' spins [41,42]. Furthermore, an all-electrical control of molecules' magnetic moments and an extreme tunnel magnetoresistance in double molecular magnets were also predicted [45,46]. Although transport properties of double molecular magnets have recently attracted certain attention, there are still several aspects that undoubtedly require further investigations.

In this paper, we in particular study the transport behavior of two, coupled in series, single molecular magnets weakly attached to external leads, focusing on the Pauli spin blockade regime. The Pauli spin blockade was observed in double quantum dot systems [47–49] and the mechanism leading to it was already extensively studied [50–56]. The blockade develops when the double dot becomes occupied by a triplet state. Then, an electron from one quantum dot cannot tunnel to the second dot, since the Pauli exclusion principle prevents from having two equal-spin electrons on the same level and, consequently, the current becomes blocked. Here, we investigate the effect of Pauli spin blockade in the case of double molecular magnets. The calculations are performed with the aid of the real-time diagrammatic technique [57] in the lowest-order perturbative expansion with respect to the tunnel coupling to the leads. Each molecule is characterized by its spin number and magnetic anisotropy. It is assumed that transport takes place through the lowest unoccupied orbital levels (LUMO) of the molecules, which are exchange-coupled to the core spins of SMMs [11,12]. We study the bias dependence of the current and the shot noise for different intrinsic parameters of magnetic molecules. We show that the Pauli spin blockade in double molecular magnets is associated with occupation of the corresponding highest-weight spin states of the system. Moreover, its range and magnitude depends greatly on the exchange interaction between the LUMO level and core spin of each molecule, as well as on the hopping between the molecules and the size of SMMs' spins. In addition, we demonstrate that contrary to double quantum dots [47], the current suppression occurs for both positive and negative bias polarization when the exchange coupling is of antiferromagnetic type. We also show that the current suppression is accompanied with a negative differential conductance and a large super-Poissonian shot noise.

The paper is organized in the following way. In Sec. II, we describe the model Hamiltonian and method used for calculations. Section III contains the numerical results on the current and shot noise, where the effects of different exchange coupling (Sec. III A), hopping between SMMs (Sec. III B), and magnitude of SMMs' spins (Sec. III C) are thoroughly discussed. The paper is summarized in Sec. IV.

II. MODEL AND METHOD

We consider a system built of two single molecular magnets coupled to each other and to external metallic leads, as sketched in Fig. 1. The molecules are modeled by giant spin Hamiltonians and it is assumed that transport of electrons occurs through the lowest unoccupied molecular orbitals of

*anna.plominska@amu.edu.pl

 ©2016 American Physical Society

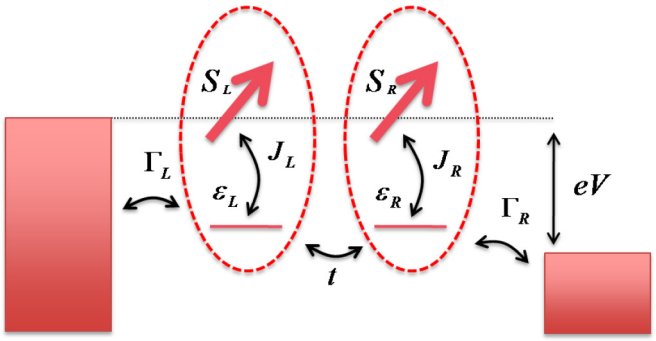

FIG. 1. Schematic of the considered system. It consists of two molecular magnets with spin S_r ($r = L, R$), coupled to each other via hopping matrix elements t and to the left and right metallic leads with coupling strengths Γ_L and Γ_R, respectively. The energy of orbital level of left (right) molecule is denoted by $\varepsilon_{L(R)}$ and $J_{L(R)}$ describes the exchange interaction between the electrons occupying given orbital level and the internal spin of given molecule. The bias voltage is applied symmetrically to the system, $\mu_L - \mu_R = eV$.

SMMs. Consequently, the total Hamiltonian has the following form:

$$H = H_{\text{Lead}} + H_{\text{DSMM}} + H_{\text{Tun}}, \tag{1}$$

where the first term describes the noninteracting electrons in the leads,

$$H_{\text{Lead}} = \sum_{r=L,R} \sum_{k\sigma} \varepsilon_{rk} c^\dagger_{rk\sigma} c_{rk\sigma}, \tag{2}$$

with $c^\dagger_{rk\sigma}$ ($c_{rk\sigma}$) being the creation (annihilation) operator of an electron with spin σ, momentum k and energy ε_{rk} in the lead r. The second term of the Hamiltonian H describes the two coupled single molecular magnets and is given by

$$H_{\text{DSMM}} = \sum_{r=L,R} H^r_{\text{SMM}} + t \sum_{\sigma} (d^\dagger_{L\sigma} d_{R\sigma} + d^\dagger_{R\sigma} d_{L\sigma}) + U'(n_{L\uparrow} + n_{L\downarrow})(n_{R\uparrow} + n_{R\downarrow}). \tag{3}$$

Here, $d^\dagger_{r\sigma}$ is the creation operator for an electron with spin σ on the molecular orbital of rth SMM with the corresponding energy ε_r, and $n_{r\sigma} = d^\dagger_{r\sigma} d_{r\sigma}$. The Coulomb correlations between the two molecules are described by U', while t denotes the hopping matrix elements between the SMMs. The Hamiltonian H^r_{SMM} models the rth SMM and is given by [11,12,30,32]

$$H^r_{\text{SMM}} = \varepsilon_r n_{r\sigma} + U_r n_{r\uparrow} n_{r\downarrow} - J_r \mathbf{S}_r \cdot \mathbf{s}_r - D_r S^2_{rz}, \tag{4}$$

where U_r describes the Coulomb correlations in the molecule, J_r is the exchange interaction between the core spin of the molecule characterized by spin operator $\mathbf{S}_r$ and spin of electron occupying the corresponding LUMO level, $\mathbf{s}_r = \frac{1}{2} \sum_{\sigma\sigma'} d^\dagger_{r\sigma} \vec{\sigma}_{\sigma\sigma'} d_{r\sigma'}$, with $\vec{\sigma}$ being the vector of Pauli spin matrices. The uniaxial magnetic anisotropy of rth SMM is described by D_r and S_{rz} is the zth component of the rth molecule's spin. Although the two molecules can, in principle, be different, for the sake of clarity, in the following we assume that they have equal spins $S_L = S_R \equiv S$ and can be modeled by the same parameters, i.e., $U_L = U_R \equiv U$, $J_L = J_R \equiv J$, and $D_L = D_R \equiv D$. The last term of the total Hamiltonian describes the tunnel-coupling between the molecular magnet dimer and the leads. It is given by

$$H_{\text{Tun}} = \sum_{r=L,R} \sum_{k\sigma} v_r (c^\dagger_{rk\sigma} d_{r\sigma} + d^\dagger_{r\sigma} c_{rk\sigma}), \tag{5}$$

where v_r denotes the respective tunnel matrix elements. The strength of the coupling between the lead r and the LUMO level of rth molecular magnet can be expressed as $\Gamma_r = 2\pi \rho_r v_r^2$, where ρ_r is the density of states of lead r. In the following, we assume that the system is symmetrically coupled, $\Gamma_L = \Gamma_R \equiv \Gamma/2$, and the voltage drop is applied symmetrically between the left and right leads, $\mu_L - \mu_R = eV$, see Fig. 1.

In this paper, we study the nonequilibrium transport properties of considered molecular magnet dimer assuming weak coupling to the leads. The current can be then calculated perturbatively in the tunnel-coupling strength Γ by employing the real-time diagrammatic technique [57–60]. In our considerations, we take into account the lowest-order of perturbation expansion, which corresponds to sequential tunneling processes. First, we need to determine the elements $W_{\chi\chi'}$ of the self-energy matrix $\mathbf{W}$, which describe transitions between many-body states $|\chi\rangle$ of the system, where $|\chi\rangle$ is an eigenstate of the double molecular magnet Hamiltonian (3), $H_{\text{DSMM}}|\chi\rangle = \varepsilon_\chi |\chi\rangle$. The off-diagonal elements of this matrix are given by [58,59]

$$W_{\chi\chi'} = \sum_{r=L,R} \left[F^r_{\chi\chi'} + \bar{F}^r_{\chi'\chi} \right], \tag{6}$$

where

$$F^r_{\chi\chi'} = 2\pi \sum_{\sigma} \rho_r f_r(\varepsilon_\chi - \varepsilon_{\chi'}) |v_r \langle \chi | d^\dagger_{r\sigma} | \chi' \rangle|^2 \tag{7}$$

and $f_r(\varepsilon) = 1/[e^{(\varepsilon-\mu_r)/T} + 1]$ is the Fermi-Dirac distribution function of lead r with μ_r denoting the corresponding electrochemical potential and the Boltzmann constant $k_B \equiv 1$. The quantity $\bar{F}^r_{\chi\chi'}$ is given by Eq. (7) with $f_r(\varepsilon)$ replaced by the hole distribution function $1 - f_r(\varepsilon)$. On the other hand, the diagonal elements of matrix $\mathbf{W}$ are given by $W_{\chi\chi} = -\sum_{\chi' \neq \chi} W_{\chi'\chi}$. In the steady state, the occupation probabilities P_χ of many-body states $|\chi\rangle$ can be found from [58,59]

$$(\tilde{\mathbf{W}}\mathbf{P})_\chi = \Gamma \delta_{\chi\chi_0}, \tag{8}$$

where $\mathbf{P}$ is the vector of probabilities and $\tilde{\mathbf{W}}$ is equal to $\mathbf{W}$ with one row corresponding to χ_0 modified so as to take into account the normalization condition. The current can be then calculated from the equation [58,59]

$$I = \frac{e}{2\hbar} \text{Tr}\{\mathbf{W}^I \mathbf{P}\}, \tag{9}$$

where

$$W^I_{\chi\chi'} = F^R_{\chi\chi'} - F^L_{\chi\chi'} + \bar{F}^L_{\chi'\chi} - \bar{F}^R_{\chi'\chi} \tag{10}$$

for off-diagonal matrix elements and $W^I_{\chi\chi'} = 0$ for $\chi = \chi'$.

In addition to the current, we also analyze the behavior of the zero-frequency shot noise, [61] $S_I = \int_{-\infty}^{\infty} dt [\langle \hat{I}(t)\hat{I}(0)\rangle + \langle \hat{I}(0)\hat{I}(t)\rangle - \langle \hat{I}\rangle^2]$, where $\hat{I}$ is the current operator. The shot noise can provide additional information about the transport

processes, which is not contained in the averaged current I. Within the real-time diagrammatic technique, S_I in the lowest-order expansion in the coupling strength Γ can be found from [58]

$$S_I = \frac{e^2}{\hbar}\mathrm{Tr}\{\mathbf{W}^{II}\mathbf{P} + \mathbf{W}^{I}\check{\mathbf{P}}\mathbf{W}^{I}\mathbf{P}\}, \tag{11}$$

where the matrix elements of $\mathbf{W}^{II}$ are given by $W^{II}_{\chi\chi'} = (1/2 - \delta_{\chi\chi'})W_{\chi\chi'}$ and the quantity $\check{\mathbf{P}}$ can be found from $\tilde{\mathbf{W}}\check{\mathbf{P}} = \mathbf{Q}$, with the elements of $\mathbf{Q}$ given by $Q_{\chi,\chi} = (P_{\chi'} - \delta_{\chi'\chi})(1 - \delta_{\chi'\chi_0})$. Having found the shot noise, we can determine the Fano factor $F = S_I/S_P$, which describes the deviation of S_I from the Poissonian shot noise given by $S_P = 2e|I|$ [61].

III. RESULTS AND DISCUSSION

To begin with, let us recall the main mechanism responsible for the occurrence of the Pauli spin blockade in serial double quantum dot systems [47,51,52]. When at equilibrium the level of the left dot is half-filled ($\varepsilon_L \approx -U/2$) while the doubly occupied state of the right dot is close to the Fermi energy of the leads ($\varepsilon_R \approx -U$), for finite capacitive coupling between the dots (here we assume $U' = U/2$) the ground state of the double dot is a delocalized spin singlet. The energy of this state is, however, very close to the energy of triplet states, single-electron states and other two-electron singlets. The corresponding excitation energies are in fact of the order of the considered thermal energy. Therefore, with increasing the bias voltage, $\mu_L - \mu_R = eV > 0$, the electrons starts tunneling from the left to the right lead. For negative bias, the first Coulomb step in the current occurs, while for positive bias, there is only a small maximum in the current, since the tunneling processes become suppressed very fast with increasing eV. This happens when the spin of electron in the left dot is the same as that of an electron occupying the right dot. The system gets then trapped in a triplet state and the current becomes blocked, since the electron from the left dot cannot tunnel to the right dot due to the Pauli exclusion principle, provided the next orbital level is not accessible for transport within the considered bias range. This blockade is referred to as the Pauli spin blockade [47]. It can be explicitly seen in Fig. 2(a), which shows the bias voltage dependence of the current calculated for different values of the hopping parameter t. When the bias voltage increases further, the current raises around $eV \approx U$, but then suddenly drops again. This suppression is now related to a full occupation of the doubly occupied state of the left dot, which forbids the electrons from the left lead to enter the left dot. The current is thus suppressed due to a charge blockade. We note that when more levels are accessible for transport in each dot, the range of bias voltage where the blockade occurs may be changed [47,53]. The situation is completely different when the voltage is reversed. For negative bias voltages, the occupation of singly occupied states increases and the blockade is lifted since tunneling due to doubly and singly occupied states is allowed. With further increase of negative bias voltage, there are next steps in the current and the $i - v$ characteristic displays typical Coulomb staircase for $eV < 0$ [9,47]. As shown theoretically [51,52], the triplet blockade can be weakened with increasing t, because the occupation of the triplet state, and thus the blockade itself, strongly depends on the ratio of $2t/\Delta\varepsilon$, where $\Delta\varepsilon = \varepsilon_L - \varepsilon_R$, see Fig. 2(a). Moreover, in the transport region where the suppression of the current due to the triplet occupation occurs, the Fano factor becomes larger than unity, indicating super-Poissonian shot noise [53,59,62–64]. This can be seen in Fig. 2(b), which displays the bias dependence of the Fano factor for different hoppings t. For reversed bias voltages, the shot noise is generally sub-Poissonian, which is typical for Coulomb-correlated sequential transport [61,65–67]. When the hopping parameter is increased, the current in the blockade regime increases. The Fano factor becomes then slightly suppressed, however, the shot noise is still super-Poissonian, see Fig. 2.

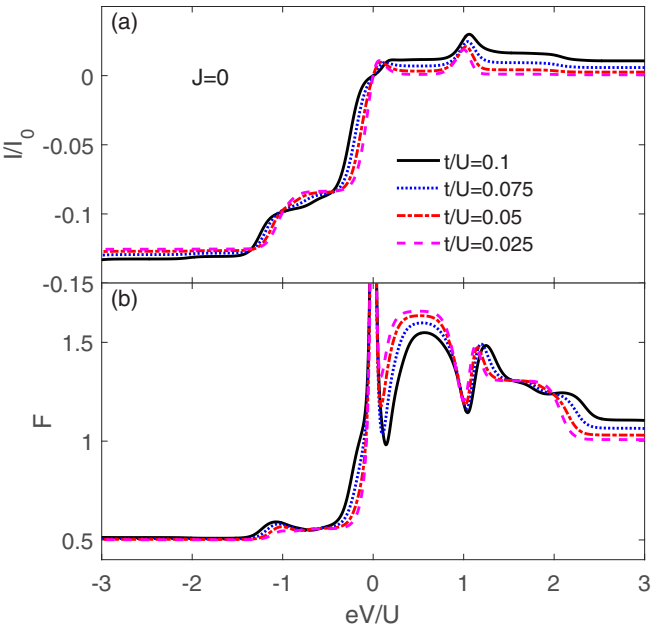

FIG. 2. The bias voltage dependence of (a) the current I and (b) the Fano factor F calculated for different values of hopping between the LUMO levels, as indicated, in the case of $J = 0$. The parameters are: $U' = -\varepsilon_L = 0.5$, $\varepsilon_R = -1$ and $T = 3\Gamma = 0.03$ in units of $U \equiv 1$. The current is plotted in units of $I_0 = e\Gamma/\hbar$.

In the following, we analyze the current and shot noise of two, coupled in series, single molecular magnets, as described by the Hamiltonian (3), focusing on the Pauli spin blockade regime. In this context, Fig. 2 will serve as a reference in understanding how the transport properties change compared to double quantum dot systems. We discuss the results in the case of both ferromagnetic and antiferromagnetic exchange coupling J between the molecules' core spins and the LUMO levels. In the former case, the total spin S_r^{tot} of rth molecule tends to be increased, $S_r^{\mathrm{tot}} = S + s$, while in the latter case, the spin is lowered $S_r^{\mathrm{tot}} = |S - s|$. As shown recently for one SMM coupled to ferromagnetic contacts [12], the type of exchange interaction can have a large impact on the current flowing through the system. Although in the considered model the leads are nonmagnetic, one can still expect a strong impact of the exchange interaction J on the transport behavior, since the blockade regime is determined by an appropriate spin configuration of the system. Therefore we study the dependence

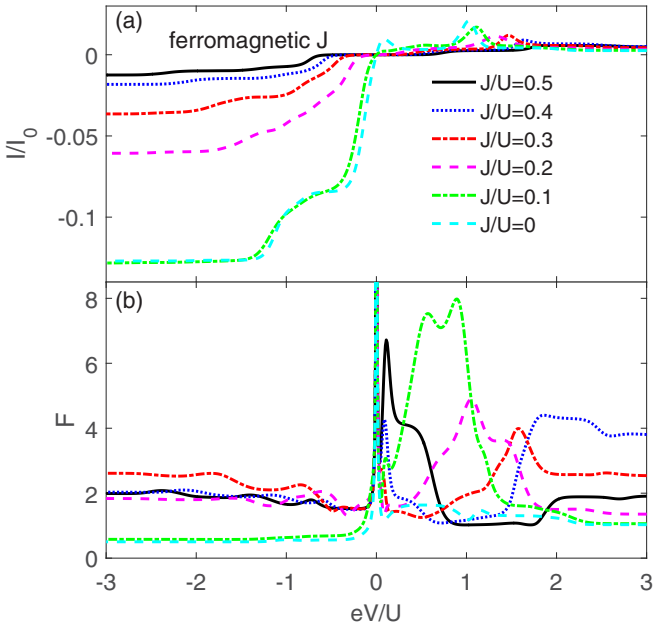

FIG. 3. The bias voltage dependence of (a) the current and (b) the Fano factor for different values of the ferromagnetic ($J > 0$) exchange coupling between the LUMO level and core spin of each molecule, as indicated. The parameters are the same as in Fig. 2 with $D/U = 0.05$, $t/U = 0.05$, and $S = 3/2$.

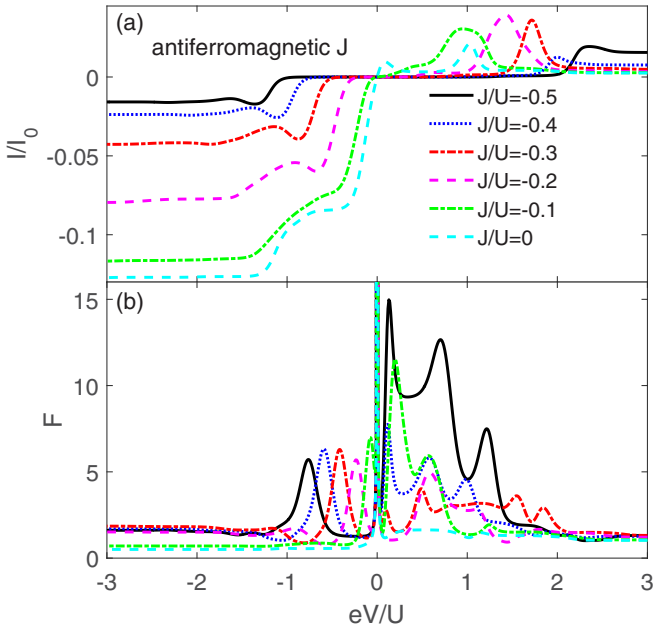

FIG. 4. The same as in Fig. 3 calculated in the case of antiferromagnetic exchange interaction ($J < 0$).

of transport characteristics on both the strength and sign of exchange interaction. We then assume constant $|J|$ and analyze the effect of different hopping between the molecular magnets. While most of the calculations are performed for hypothetical molecules with spin $S = 3/2$ [2,68] and uniaxial magnetic anisotropy $D/U = 0.05$, we eventually also consider the effect of different SMM spin on transport properties. We would also like to emphasize that the two molecules are assumed to be equal and the asymmetry necessary to obtain asymmetric i-v characteristics is introduced by finite orbital level detuning, which can be experimentally realized by appropriate gating.

A. The effects of different exchange coupling J

The bias voltage dependence of the current and Fano factor for different values of exchange interaction J between the LUMO level and the SMM core spin S is shown in Fig. 3. This figure was calculated in the case of ferromagnetic type of exchange interaction, while the corresponding case with antiferromagnetic J is displayed in Fig. 4. Let us first discuss the behavior in the case of $J > 0$. For relatively small values of J, see the curves for $J/U \leqslant 0.1$ in Fig. 3(a), the bias dependence is similar to the double quantum dot case shown in Fig. 2. However, after a closer inspection, one can see that in the case of finite J there is no negative differential conductance associated with the spin blockade, although the current is still suppressed. In fact, NDC is only present for very low values of J, $J/U \lesssim 0.1$. On the other hand, the second NDC associated with the maximum in the current around $eV/U \approx 1$ does not disappear with increasing J, but only moves toward larger values of eV. Interestingly, for finite J, a large current suppression occurs also for negative bias voltage. Nevertheless, this suppression is not associated with negative differential conductance, which is present only for positive bias voltage, see Fig. 3(a).

To understand the behavior of the current in the case of finite J, in Fig. 5 we show the bias dependence of the expectation values of the SMM's occupation numbers, $n_r = \sum_\sigma n_{r\sigma}$,

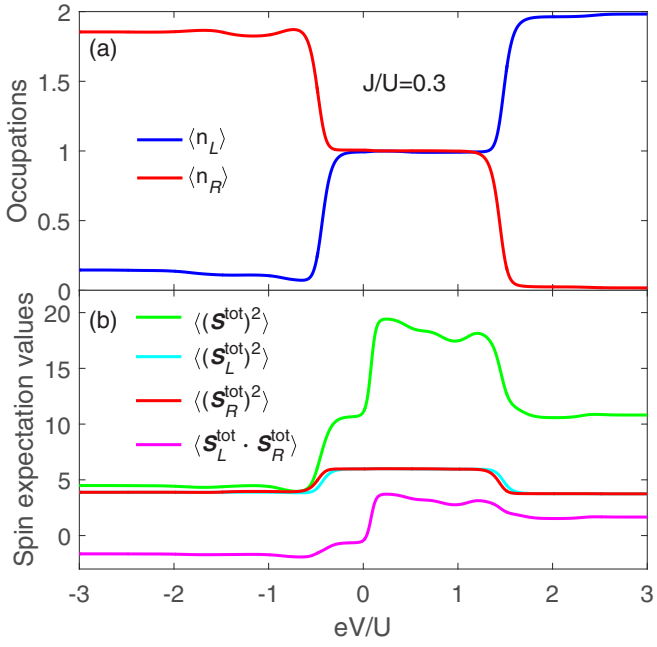

FIG. 5. The bias voltage dependence of (a) the expectations values of the left and right SMM's occupation, $\langle n_L \rangle$ and $\langle n_R \rangle$, and (b) the corresponding spin expectation values calculated in the case of ferromagnetic exchange interaction, $J/U = 0.3$. The other parameters are the same as in Fig. 3.

the spin operator of each molecule $\mathbf{S}_r^{\rm tot} = \mathbf{S}_r + \mathbf{s}_r$, the total spin of double molecular magnet $\mathbf{S}^{\rm tot} = \mathbf{S}_L^{\rm tot} + \mathbf{S}_R^{\rm tot}$, and the expectation value of $\langle \mathbf{S}_L^{\rm tot} \cdot \mathbf{S}_R^{\rm tot} \rangle$. This figure was calculated for one selected value of J, namely, $J/U = 0.3$. First, let us recall that for ferromagnetic exchange interaction, the total spin of each molecule is increased, $S_r^{\rm tot} = S + s$. However, the total spin of double molecular magnet $S^{\rm tot}$ depends on the effective exchange interaction between the molecules, J_{LR}, which is generated by finite hopping t. Depending on the bias voltage and parameters, the sign of $J_{LR} \propto \langle \mathbf{S}_L^{\rm tot} \cdot \mathbf{S}_R^{\rm tot} \rangle$ can change. As can be seen in Fig. 5(b), for positive bias voltage, ranging from zero to the first maximum around $eV/U \approx 1$, $\langle \mathbf{S}_L^{\rm tot} \cdot \mathbf{S}_R^{\rm tot} \rangle > 0$ and consequently J_{LR} is of ferromagnetic type. The total spin of double molecular magnet is then enhanced to $S^{\rm tot} = 2(S + s)$ and the system is trapped in the highest-weight spin states, $|n_{\rm tot}, S_z^{\rm tot}\rangle = |2, \pm 2(S + s)\rangle$, where $n_{\rm tot} = \sum_r n_r$ is the total electron number, while $S_z^{\rm tot}$ is the zth component of the total spin. Because of that, the tunneling of electrons through the LUMO levels is blocked. With increasing the bias voltage, a small maximum in the current occurs, see Fig. 3(a). This is due to finite occupancy of single electron states $|1, \pm(2S + s)\rangle$, which allow for sequential transport processes through the system. However, further increase of the bias voltage results again in the current suppression and associated NDC. This behavior results from an enhanced occupancy of two-electron states $|2, \pm 2S\rangle$, with the LUMO level of the left molecule doubly occupied and the right molecule being empty, see Fig. 5(a). In this case, the electrons from the left lead cannot tunnel to the left SMM and the current becomes suppressed. This scenario holds for finite ferromagnetic exchange interaction $J/U \gtrsim 0.1$, see Fig. 3(a). As can be seen in the figure, increasing J results only in a change of the range of bias voltage where the two blockades occur, while the mechanisms responsible for those current suppressions remain the same.

As can be seen in Fig. 3(a), for negative bias voltage the current decreases with increasing the exchange interaction J. This suppression is associated with an enhanced occupation of the two electron states $|2, 0\rangle$, with two electrons occupying the right LUMO level, see Fig. 5(a). In the following we will refer to the states with $S_z^{\rm tot} = 0$ as to singlet states. In such a case, the current is blocked because no electron can tunnel to the right SMM from the right lead. This current suppression is thus very similar to the one occurring for positive bias voltage for $eV \gtrsim U$. The fact that the blockade for negative bias voltage is not perfect is associated with finite occupation of other molecular states, which allow for tunneling of electrons through the system. We also note that for negative bias voltage, $\langle \mathbf{S}_L^{\rm tot} \cdot \mathbf{S}_R^{\rm tot} \rangle < 0$, and the effective exchange interaction between SMMs is of antiferromagnetic type, see Fig. 5(b). Consequently, the system is mostly occupied by two-electron singlet states.

Different transport behavior is also revealed in the bias voltage dependence of the Fano factor, which is shown in Fig. 3(b). When $F = 1$, the shot noise is Poissonian and transport is due to uncorrelated-in-time tunneling events [61]. In the sequential tunneling regime, the shot noise is typically sub-Poissonian with $F < 1$, since tunneling processes are correlated by the charging energy [65,66]. On the other hand, super-Poissonian shot noise ($F > 1$) may occur in transport

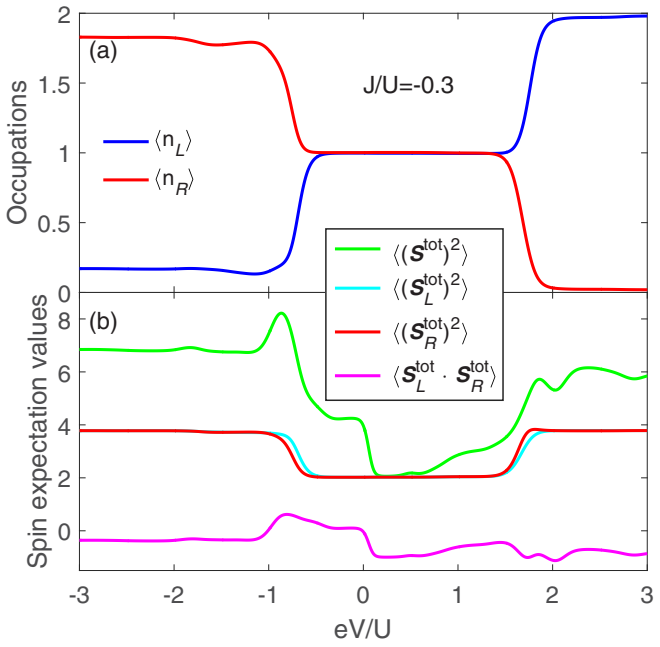

FIG. 6. The same as in Fig. 5 calculated for $J/U = -0.3$.

regions where the current is suppressed by trapping the system in certain states, which gives rise to large current fluctuations [53,59,64]. One should also note that F becomes infinite at zero bias, since the current then vanishes, while the shot noise is given by thermal noise [61]. All these values of the Fano factor can be observed in the bias dependence of F displayed in Fig. 3(b). We first note that when J is finite, the shot noise is much enhanced compared to the double dot case shown in Fig. 2. Moreover, for considerable exchange interaction J, large current fluctuations can be observed in the whole range of considered bias voltage, see Fig. 3(b). For positive bias voltage, the shot noise is generally super-Poissonian with $F \gtrsim 1$, irrespective of the value of J. The current is there suppressed due to either trapping in high-spin states or by Coulomb correlations and size quantization. For negative bias voltage, when $J/U \lesssim 0.1$, which corresponds to the situation when the spins S are relatively weakly coupled to LUMO levels, the shot noise is sub-Poissonian with $F \approx 1/2$, which is characteristic of sequential tunneling transport regime. Nevertheless, with increasing the value of J, the current becomes suppressed and the system exhibits super-Poissonian shot noise, see the curves for $J/U > 0.1$ in Fig. 3(b). However, despite the above general observations, the dependence of F on eV for a particular value of J is very complex. In particular, inside the blockade regimes a large super-Poissonian shot noise can be observed for certain bias voltages. The range of bias voltage changes with increasing J, such that for fixed eV the Fano factor varies in a nonmonotonic way with J, see Fig. 3(b).

The bias voltage dependence of the current and Fano factor in the case when the exchange interaction between the LUMO level and core spin of each molecule is of antiferromagnetic type is shown in Fig. 4, while the corresponding expectation values calculated for $J/U = -0.3$ are shown in Fig. 6. Now, $J < 0$ tends to lower the spin of each molecule, such that

$S_r^{\rm tot} = |S - s|$, see Fig. 6(b). Consequently, transport does not occur through highest-weight spin states, but through molecular states with lower spin values. First, we note that similar to the ferromagnetic-J case, when $|J|/U \gtrsim 0.1$, the current is suppressed with increasing the bias voltage, but there is no negative differential conductance around the zero bias, see Fig. 4(a). This suppression is now related to an enhanced occupation of singlet states $|2,0\rangle$ with two electrons occupying different LUMO levels (singlet forms between electrons occupying LUMO levels), which increases with raising $|J|$ ($J < 0$). At some finite bias voltage, the current exhibits a maximum, which moves toward larger eV with increasing J. This maximum is associated with a relatively low but finite occupation of one-electron states. Nevertheless, with further increase of the bias voltage, again the two-electron states become mainly populated, but now with two electrons occupying the left LUMO level, see Fig. 6(a). This effectively blocks tunneling through the system and the current drop is accompanied with a pronounced NDC, see Fig. 4(a). This situation is qualitatively similar to the case of ferromagnetic exchange interaction. The current blockade is accompanied by large current fluctuations, with $F > 10$ in the case of $J/U = -0.5$, see Fig. 4(b). The bias dependence of F is however more systematic compared to the ferromagnetic-J case. At low bias voltage, the Fano factor generally increases with raising $|J|$, while for larger bias voltages, F only slightly depends on J and takes values slightly exceeding unity.

When the bias voltage is reversed and the antiferromagnetic coupling between the LUMO level and core spin of each molecule becomes strong, the system exhibits negative differential conductance, see Fig. 4(a). At low bias voltage the system is occupied by the states $|2,0\rangle$ and $|2,\pm(S-s)\rangle$, with each LUMO level being singly occupied, and the current is blocked, see Fig. 6. The range of bias voltage where this is the case extends with increasing J. When the bias voltage is lowered further, one-electron states become available for transport and the current starts increasing. However, this is accompanied by gradual enhancement of occupation of two-electron singlet states $|2,0\rangle$, with two electrons located in the right molecule [cf. Fig. 6(a)], which results in the current suppression again. Consequently, it leads to a small maximum in the absolute value of the current and considerable negative differential conductance, see Fig. 4(a). As can be clearly seen in the figure, the current suppression is enhanced with increasing $|J|$. Moreover, NDC occurs when the coupling between the LUMO level and core spin is relatively strong, see the curves for $J/U \lesssim -0.2$ in Fig. 4(a). In the suppression regime, where NDC is present, the shot noise is super-Poissonian with $F \approx 1.5$, see Fig. 4(b), and otherwise, for $|J|/U \lesssim 0.1$, the shot noise is sub-Poissonian. We also note that the Fano factor exhibits a maximum with $F \approx 6$ at low bias voltages for any finite value of J. This maximum occurs just at the onset of step in the current, see Fig. 4(b). As already mentioned above, the system is then mostly occupied by states $|2,0\rangle$ and $|2,\pm(S-s)\rangle$ with one electron on each molecule. However, when the voltage approaches the threshold value, there is a small finite occupation of single-electron states, which allow for the current flow and result in large current fluctuations.

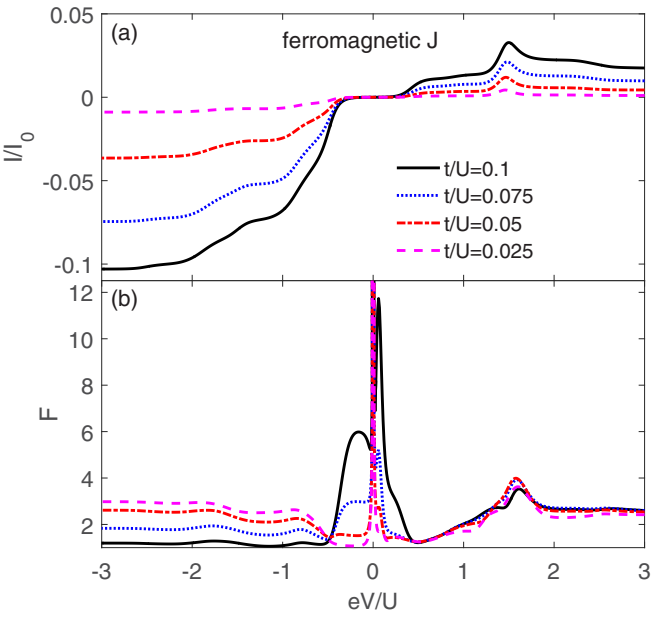

FIG. 7. The bias voltage dependence of (a) the current and (b) the Fano factor for different values of the hopping parameter t, as indicated, in the case of ferromagnetic exchange interaction. The parameters are the same as in Fig. 3 with $J/U = 0.3$.

We note that the shot noise in the Pauli spin blockade regime is super-Poissonian even for $J = 0$, however, its value reaches $F \approx 1.6$, cf. Fig. 2(b). On the other hand, when the exchange coupling J is finite, the shot noise becomes much enhanced, irrespective of the type of exchange interaction. Moreover, contrary to the double dot case, the shot noise becomes super-Poissonian for reversed bias voltage, cf. Figs. 3(b) and 4(b). We notice that a very large super-Poissonian shot noise was predicted recently in a system consisting of a quantum dot spin valve with an attached magnetic impurity [68].

B. The effect of different hopping between SMMs

In this section, we analyze how changing the hopping between the molecular magnets affects the transport characteristics. In analysis we assume constant exchange interaction between the LUMO level and core spin of each molecule, $|J|/U = 0.3$. The bias voltage dependence of the current and Fano factor for different values of t in the case of ferromagnetic exchange interaction is shown in Fig. 7, while Fig. 8 presents the transport behavior in the case of antiferromagnetic exchange interaction. The first observation is that the current depends monotonically on t and becomes generally suppressed with decreasing the value of hopping t. Contrary to the double dot case [cf. Fig. 2(a)], now the suppression occurs both in the Pauli spin blockade regime for positive bias as well as for negative bias voltage. While the bias voltage dependence for $eV > 0$ is qualitatively similar to the case of ferromagnetic and antiferromagnetic J, with a maximum in the current around $eV/U \approx 1.6$, which increases with increasing t, this is not the case for $eV < 0$. For negative bias voltage, when $J > 0$, the current varies monotonically with eV, whereas for $J < 0$, the dependence is nonmonotonic when $t/U \lesssim 0.075$, see Figs. 7(a) and 8(a). This difference can be understood by

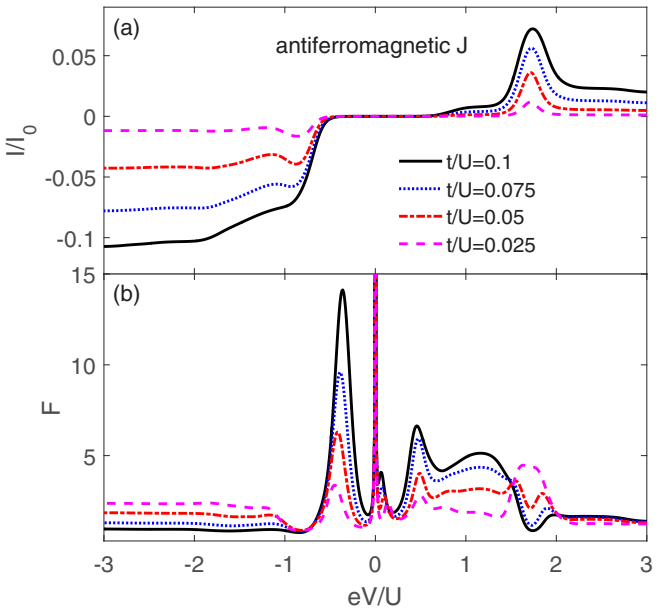

FIG. 8. The same dependence as in Fig. 7 calculated in the case of antiferromagnetic exchange interaction $J/U = -0.3$.

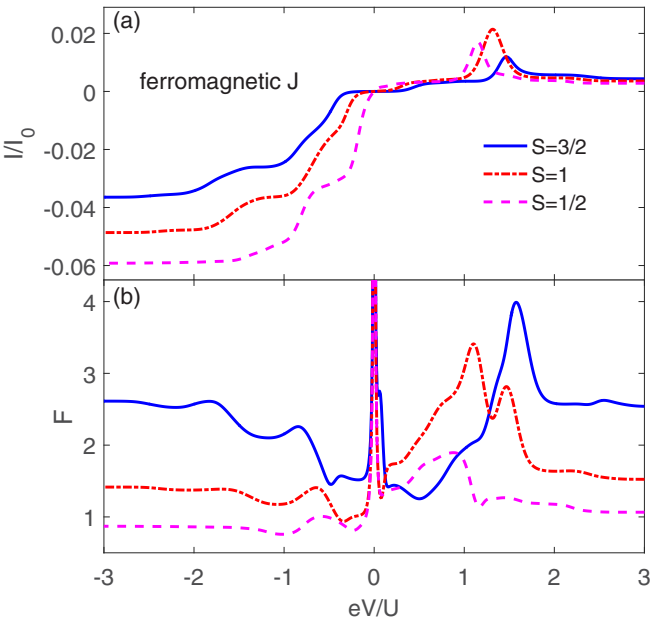

FIG. 9. The dependence of (a) the current and (b) the Fano factor on the applied bias voltage calculated in the case of ferromagnetic exchange interaction for different values of SMM spin S. The parameters are the same as in Fig. 3 with $J/U = 0.3$.

analyzing different states taking part in transport. In the case of ferromagnetic exchange interaction, for negative bias the system is mainly occupied by two two-electron singlet states with doubly occupied right dot. There is also relatively small occupation of one-electron states, which enable for tunneling through the system. On the other hand, in the case of $J < 0$, at low negative bias voltage the system is occupied by two states $|2,\pm 2(S-s)\rangle$ with two electrons on the right molecule. When the voltage is lowered, just after the step in the current, the system becomes mainly occupied by one singlet state $|2,0\rangle$, again with two electrons occupying the right molecule. Because of that, the current becomes suppressed and the system exhibits negative differential conductance. The NDC disappears with increasing t, see the curve for $t/U = 0.1$ in Fig. 8(a), because the occupation of the singlet state decreases with t.

Let us now discuss the behavior of the Fano factor. For ferromagnetic exchange interaction and positive bias voltage, the Fano factor hardly depends on the magnitude of t. The only dependence can be visible around the zero bias voltage, where F exhibits a peak for $t/U = 0.1$, see Fig. 7(b). For negative bias voltage, the dependence on t is already more pronounced. One can see that in the low bias voltage regime where the current is suppressed, the shot noise takes super-Poissonian values and F becomes enhanced with increasing t. When finite current flows through the system, this dependence is just opposite. For large t, the shot noise is sub-Poissonian and becomes super-Poissonian with decreasing the value of t. The current suppression with t reveals thus in an enhanced shot noise, see Fig. 7(b). When the exchange interaction J is antiferromagnetic, the shot noise depends strongly on t for both positive and negative bias voltages. In the spin blockade regime, the Fano factor exceeds unity for all values of t considered and increases with raising the hopping t, see Fig. 8(b). For voltages where the maximum in the current occurs, this dependence is opposite, i.e., Fano factor decreases with increasing t. On the other hand, in the blockade region for $eV/U \gtrsim 2$, F very weakly depends on t. Qualitatively, similar behavior can be observed for negative bias voltage. The Fano factor increases (decreases) with increasing t in the blockade regime (out of the blockade regime, for $eV/U \lesssim -0.6$), see Fig. 8(b).

C. The effect of different spin of SMMs

Finally, we study the bias dependence of the current and Fano factor for different values of molecules' spin S. The corresponding transport characteristics are shown in Figs. 9 and 10 for the case of ferromagnetic and antiferromagnetic J, respectively. These curves were calculated assuming $t/U = 0.05$ and $|J|/U = 0.3$. In the case of ferromagnetic exchange interaction, for positive bias voltage, the system is occupied by the highest-weight two-electron states and the current is suppressed. The suppression region clearly depends on the magnitude of SMM spin S. First of all, with increasing S, the low bias voltage regime where the current is suppressed becomes extended. This can be seen as a gradual shift of the maximum in the current for positive bias to larger values of eV, and an increase of the absolute value of the threshold voltage for negative bias, see Fig. 9(a). Moreover, for $eV < 0$, increasing S results in a general suppression of the current. To understand this behavior, we recall that in this transport regime the system is mainly occupied by singlet states $|2,0\rangle$ with two electrons on the right molecule. There is also some finite occupation of one-electron states (with one electron on the right SMM) and three-electron states (with one electron on the left molecule and two electrons on the right one). Increasing the value of S leads to an increase of occupation of two-electron singlet states at the cost of one and three-electron

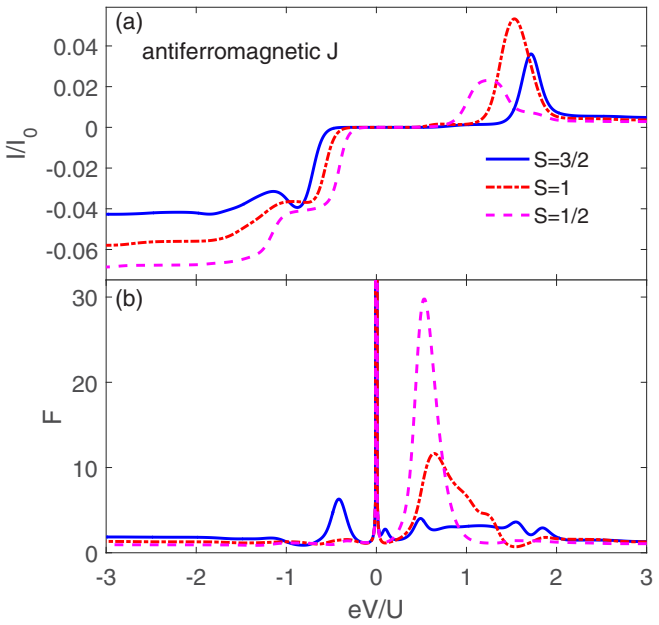

FIG. 10. The same dependence as in Fig. 9 calculated for antiferromagnetic exchange interaction $J/U = -0.3$ between the LUMO level and molecule's core spin.

states. Consequently, the current becomes suppressed when the molecules have larger spin, see Fig. 9(a). A similar tendency can be observed in the case of antiferromagnetic exchange interaction, see Fig. 10(a). The mechanism leading to the corresponding behavior of the current was already discussed in previous sections and will not be repeated here. However, we would like to notice that while negative differential conductance for positive bias is always present, for negative bias it occurs only for molecules with large enough spin, see the curve for $S = 3/2$ in Fig. 10(a).

As far as the Fano factor is concerned, in the case of ferromagnetic exchange interaction, increasing the spin of the molecules results in a general enhancement of current fluctuations, see Fig. 9(b). For negative bias, the noise is super-Poissonian when $S \geqslant 1$, while for positive bias voltage, $F \gtrsim 1$ for all values of S considered. The maximum Fano factor $F \approx 4$ occurs in the case of $S = 3/2$ for positive bias around the maximum in the current. When the exchange interaction between the LUMO level and core spin of each SMM is of antiferromagnetic type, we observe a greatly enhanced Fano factor, see Fig. 10(b). First, there is an enhancement of the shot noise in the low bias voltage regime for $eV < 0$, especially in the case of $S = 3/2$. The reason for this behavior is related to the fact that when the spin is increased, the occupation of one-electron states is lowered and the fluctuations of the current increase. Second, there is a large super-Poissonian shot noise in the blockade regime for $eV > 0$, but now it occurs for $S = 1/2$ and decreases with increasing the spin of SMMs, see Fig. 10(b). In the case of $S = 1/2$, for $J < 0$, the total spin of each molecule is a singlet and, consequently, at low bias voltage the system is fully occupied by one singlet state $|2,0\rangle$, with one electron on each LUMO level. When the bias voltage is increased, this occupation slowly decreases and thermally-activated transport processes occur. However, since the occupation of this singlet state is still close to unity, it results in large current fluctuations. On the other hand, when the spin S is larger, at zero bias there is a finite occupation of more than just a single state. Consequently, the shot noise is still super-Poissonian, but the Fano factor takes smaller values with increasing S.

IV. SUMMARY

We have studied the transport properties of two single molecular magnets in serial geometry weakly coupled to external leads. Each molecule was modeled by a single orbital level exchange-coupled to the core spin of the molecule exhibiting uniaxial magnetic anisotropy. The calculations were performed by using the real-time diagrammatic technique in the lowest order of perturbative expansion with respect to the tunnel coupling. We focused on the transport regime where the current flowing through the system was blocked by the Pauli exclusion principle. When the spins of electrons occupying the LUMO level of each molecule were the same, the electron tunneling through the system became suppressed. In the case of a double molecular magnet, the current suppression was triggered by appropriate occupation of the high-spin molecular states of the system.

In particular, we studied how transport properties in the Pauli spin blockade regime depend on both the sign and strength of exchange interaction J between the LUMO level and core spin of each molecule, as well as on the hopping between the molecules and the magnitude of SMMs' spin. We showed that, depending on intrinsic parameters of double molecular magnet, the blockade could be greatly modified. First, negative differential conductance due to the Pauli blockade effect was not present for large exchange interaction, although the current was still suppressed. Second, we found that the current could be also suppressed when the bias voltage was reversed, and this suppression was accompanied by NDC when J was of antiferromagnetic type. Moreover, we showed that in the transport regime where the current suppression occurred, the shot noise was super-Poissonian and the Fano factor could take fairly large values.

ACKNOWLEDGMENTS

This work was supported by the National Science Centre, Poland, Project No. DEC-2013/10/E/ST3/00213.

[1] A. R. Rocha, V. M. Garcia-suarez, S. W. Bailey, C. J. Lambert, J. Ferrer, and S. Sanvito, Nat. Mater. **4**, 335 (2005).

[2] D. Gatteschi, R. Sessoli, and J. Villain, *Molecular Nanomagnets* (Oxford University Press, New York, 2006).

[3] L. Bogani and W. Wernsdorfer, Nat. Mater. **7**, 179 (2008).

[4] S. Andergassen, V. Meden, H. Schoeller, J. Splettstoesser, and M. R. Wegewijs, Nanotechnol. **21**, 272001 (2010).

[5] S. Sanvito, Chem. Soc. Rev. **40**, 3336 (2011).

[6] M. N. Leuenberger and D. Loss, Nature (London) **410**, 789 (2001).

[7] D. D. Awschalom, D. Loss, and N. Samarth, *Semiconductor Spintronics and Quantum Computation* (Springer, Berlin 2002).

[8] D. Stepanenko, M. Trif, and D. Loss, Inorg. Chim. Acta **361**, 3740 (2008).

[9] H. Grabert and M. H. Devoret, *Single Charge Tunneling: Coulomb Blockade Phenomena in Nanostructures*, NATO ASI Series B: Physics Vol. 294 (Plenum Press, New York, 1992).

[10] M.-H. Jo, J. E. Grose, K. Baheti, M. M. Deshmukh, J. J. Sokol, E. M. Rumberger, D. N. Hendrickson, J. R. Long, H. Park, and D. C. Ralph, Nano Lett. **6**, 2014 (2006).

[11] C. Timm and F. Elste, Phys. Rev. B **73**, 235304 (2006).

[12] M. Misiorny, I. Weymann, and J. Barnaś, Phys. Rev. B **79**, 224420 (2009).

[13] C. Romeike, M. R. Wegewijs, W. Hofstetter, and H. Schoeller, Phys. Rev. Lett. **96**, 196601 (2006).

[14] C. Romeike, M. R. Wegewijs, W. Hofstetter, and H. Schoeller, Phys. Rev. Lett. **97**, 206601 (2006).

[15] A. F. Otte, M. Ternes, K. von Bergmann, S. Loth, H. Brune, C. P. Lutz, C. F. Hirjibehedin, and A. J. Heinrich, Nat. Phys. **4**, 847 (2008).

[16] J. J. Parks, A. R. Champagne, T. A. Costi, W. W. Shum, A. N. Pasupathy, E. Neuscamman, S. Flores-Torres, P. S. Cornaglia, A. A. Aligia, C. A. Balseiro, G. K. L. Chan, H. D. Abruna, and D. C. Ralph, Science **328**, 1370 (2010).

[17] F. Elste and C. Timm, Phys. Rev. B. **81**, 024421 (2010).

[18] M. Misiorny, I. Weymann, and J. Barnaś, Phys. Rev. Lett. **106**, 126602 (2011); Phys. Rev. B **84**, 035445 (2011).

[19] G. Christou, Polyhedron **24**, 2065 (2005).

[20] H. B. Heersche, Z. de Groot, J. A. Folk, H. S. J. van der Zant, C. Romeike, M. R. Wegewijs, L. Zobbi, D. Barreca, E. Tondello, and A. Cornia, Phys. Rev. Lett. **96**, 206801 (2006).

[21] F. Meier, L. H. Zhou, J. Wiebe, and R. Wiesendanger, Science **320**, 82 (2008).

[22] C. Iacovita, M. V. Rastei, B. W. Heinrich, T. Brumme, J. Kortus, L. Limot, and J. P. Bucher, Phys. Rev. Lett. **101**, 116602 (2008).

[23] L. Zhu, K. L. Yao, and Z. L. Liu, Appl. Phys. Lett. **96**, 082115 (2010).

[24] D. Serrate, P. Ferriani, Y. Yoshida, S.-W. Hla, M. Menzel, K. von Bergmann, S. Heinze, A. Kubetzka, and R. Wiesendanger, Nat. Nanotechnol. **5**, 350 (2010).

[25] S. Loth, K. von Bergmann, M. Ternes, A. F. Otte, C. P. Lutz, and A. J. Heinrich, Nat. Phys. **6**, 340 (2010).

[26] E. Burzuri, A. S. Zyazin, A. Cornia, and H. S. J. van der Zant, Phys. Rev. Lett. **109**, 147203 (2012).

[27] E. Burzuri, R. Gaudenzi, and H. S. J. van der Zant, J. Phys.: Condens. Matt. **27**, 113202 (2015).

[28] P. Jacobson, T. Herden, M. Muenks, G. Laskin, O. Brovko, V. Stepanyuk, M. Ternes, and K. Kern, Nat. Commun. **6**, 8536 (2015).

[29] M. Misiorny, E. Burzuri, R. Gaudenzi, K. Park, M. Leijnse, M. R. Wegewijs, J. Paaske, A. Cornia, and H. S. J. van der Zant, Phys. Rev. B **91**, 035442 (2015).

[30] F. Elste and C. Timm, Phys. Rev. B **73**, 235305 (2006).

[31] M. R. Wegewijs, C. Romeike, H. Schoeller, and W. Hofstetter, New J. Phys. **9**, 344 (2007).

[32] M. Misiorny and J Barnaś, Phys. Rev. B **75**, 134425 (2007); **76**, 054448 (2007); **77**, 172414 (2008).

[33] H.-Z. Lu, B. Zhou, and S.-Q. Shen, Phys. Rev. B **79**, 174419 (2009).

[34] R-Q Wang, L. Sheng, R. Shen, B. Wang, and D. Y. Xing, Phys. Rev. Lett. **105**, 057202 (2010).

[35] M. Misiorny, I. Weymann, and J. Barnaś, Phys. Rev. B **86**, 035417 (2012); M. Misiorny and J. Barnaś, Phys. Rev. Lett. **111**, 046603 (2013); M. Misiorny and I. Weymann, Phys. Rev. B **90**, 235409 (2014).

[36] M. Misiorny, M. Hell, and M. Wegewijs, Nat. Phys. **9**, 801 (2013).

[37] A. J. White, A. Migliore, M. Galperin, and A. Nitzan, J. Chem. Phys. **138**, 174111 (2013).

[38] A. Migliore and A. Nitzan, J. Am. Chem. Soc. **135**, 9420 (2013).

[39] B. Xu and Y. Dub, J. Phys.: Condens. Matter **27**, 263202 (2015).

[40] J.-M. Hu, Z.-D. Chen, and S.-Q. Shen, Phys. Rev. B **68**, 104407 (2003).

[41] M. Urdampilleta, S. Klyatskaya, J. P. Cleuziou, M. Ruben, and W. Wernsdorfer, Nat. Mater **10**, 502 (2011).

[42] M. Urdampilleta, N. V. Nguyen, J. P. Cleuziou, S. Klyatskaya, M. Ruben, and W. Wernsdorfer, Int. J. Mol. Sci. **12**, 6656 (2011).

[43] L. Jiang, Y. Ju, X. Liu, Z. Zhang, R. Shen, and B. Wang, Phys. Lett. A **377**, 997 (2013).

[44] L. Jiang, X. Liu, Z. Zhang, and R. Wang, Phys. Lett. A **378**, 426 (2014).

[45] N. Xue, H. Xie, Z. Wang, and J. Q. Liang, RSC Adv. **4**, 62337 (2014).

[46] T. Saygun, J. Bylin, H. Hammar, and J. Fransson, Nano Lett. **16**, 2824 (2016).

[47] K. Ono, D. G. Austing, Y. Tokura, and S. Tarucha, Science **297**, 1313 (2002).

[48] M. R. Buitelaar, J. Fransson, A. L. Cantone, C. G. Smith, D. Anderson, G. A. C. Jones, A. Ardavan, A. N. Khlobystov, A. A. R. Watt, K. Porfyrakis, and G. A. D. Briggs, Phys. Rev. B **77**, 245439 (2008).

[49] H. W. Liu, T. Fujisawa, Y. Ono, H. Inokawa, A. Fujiwara, K. Takashina, and Y. Hirayama, Phys. Rev. B **77**, 073310 (2008).

[50] H. W. Liu, T. Fujisawa, T. Hayashi, and Y. Hirayama, Phys. Rev. B **72**, 161305 (2005).

[51] J. Fransson and M. Rasander, Phys. Rev. B **73**, 205333 (2006).

[52] B. Muralidharan and S. Datta, Phys. Rev. B **76**, 035432 (2007).

[53] I. Weymann, Phys. Rev. B **78**, 045310 (2008).

[54] F. Qassemi, W. A. Coish, and F. K. Wilhelm, Phys. Rev. Lett. **102**, 176806 (2009).

[55] W. A. Coish and F. Qassemi, Phys. Rev. B **84**, 245407 (2011).

[56] J. Danon, X. Wang, and A. Manchon, Phys. Rev. Lett. **111**, 066802 (2013).

[57] H. Schoeller and G. Schön, Phys. Rev. B **50**, 18436 (1994).

[58] A. Thielmann, M. H. Hettler, J. König, and G. Schön, Phys. Rev. B **68**, 115105 (2003).

[59] A. Thielmann, M. H. Hettler, J. König, and G. Schön, Phys. Rev. B **71**, 045341 (2005).

[60] A. Thielmann, M. H. Hettler, J. König, and G. Schön, Phys. Rev. Lett. **95**, 146806 (2005).

[61] Ya. M. Blanter and M. Büttiker, Phys. Rep. **336**, 1 (2000).
[62] R. Lopez, R. Aguado, and G. Platero, Phys. Rev. B **69**, 235305 (2004).
[63] S. Gustavsson, R. Leturcq, B. Simovic, R. Schleser, P. Studerus, T. Ihn, K. Ensslin, D. C. Driscoll, and A. C. Gossard, Phys. Rev. B **74**, 195305 (2006).
[64] H. B. Xue, Z. X. Zhang, and H. M. Fei, Eur. Phys. J. B **85**, 336 (2012).
[65] E. Onac, F. Balestro, B. Trauzettel, C. F. J. Lodewijk, and L. P. Kouwenhoven, Phys. Rev. Lett. **96**, 026803 (2006).
[66] I. Weymann, J. Barnaś, and S. Krompiewski, Phys. Rev. B **76**, 155408 (2007).
[67] B. Sothmann and J. König, Phys. Rev. B **82**, 245319 (2010).
[68] S. Mossin, L. Tran, D. Adhikar, M. Pink, F. W. Heinemann, J. Sutter, R. K. Szilagyi, K. Meyer, and D. J. Mindiola, J. Am. Chem. Soc. **134**, 13651 (2012).